Commun. Comput. Phys.
doi: 10.4208/cicp.OA-2023-0233

Vol. **36**, No. 1, pp. 221-247
July 2024

The Lowest-Order Stabilized Virtual Element Method for the Stokes Problem

Xin Liu[1,2], Qixuan Song[1], Yu Gao[3] and Zhangxin Chen[4]*

[1] *School of Mathematics and Statistics, Northwestern Polytechnical University, Xi'an, 710129, China.*

[2] *MOE Key Laboratory for Complexity Science in Aerospace, Northwestern Polytechnical University, Xi'an, 710129, China.*

[3] *Department of Basic Courses, Shaanxi Railway Institute, Weinan, 714000, China.*

[4] *Department of Chemical and Petroleum Engineering, Schulich School of Engineering, University of Calgary, 2500 University Drive N.W., Calgary, Alberta T2N 1N4, Canada.*

Received 28 August 2023; Accepted (in revised version) 29 March 2024

Abstract. In this paper, we develop and analyze two stabilized mixed virtual element schemes for the Stokes problem based on the lowest-order velocity-pressure pairs (i.e., a piecewise constant approximation for pressure and an approximation with an accuracy order $k=1$ for velocity). By applying local pressure jump and projection stabilization, we ensure the well-posedness of our discrete schemes and obtain the corresponding optimal H^1- and L^2-error estimates. The proposed schemes offer a number of attractive computational properties, such as, the use of polygonal/polyhedral meshes (including non-convex and degenerate elements), yielding a symmetric linear system that involves neither the calculations of higher-order derivatives nor additional coupling terms, and being parameter-free in the local pressure projection stabilization. Finally, we present the matrix implementations of the essential ingredients of our stabilized virtual element methods and investigate two- and three-dimensional numerical experiments for incompressible flow to show the performance of these numerical schemes.

AMS subject classifications: 65N30, 65N12, 65N15, 76D05

Key words: Stokes equations, stabilized virtual element scheme, pressure jump, pressure projection, polygonal meshes.

*Corresponding author. *Email addresses:* `zhachen@ucalgary.ca` (Z. Chen), `liuxinjy@gmail.com` (X. Liu), `qixuan_song@mail.nwpu.edu.cn` (Q. Song), `gy19890524@163.com` (Y. Gao)

1 Introduction

Incompressible Stokes flow, as one of the most important and valuable problems, involves many practical applications, such as oil exploration, pipeline transportation, sedimentation, modeling of bio-suspensions, construction of efficient fibrous filters, and development of energy efficient micro-fluidic devices. Due to the limitations of fluid experiments, using computer-based numerical simulation remains an effective and flexible method in practical applications. The classical finite element method, especially with the lowest-order conforming pair (i.e., piecewise linear/bilinear C^0 velocities and piecewise constant pressures) with convenient construction (i.e., simpler shape functions) and fast implementation (i.e., fewer degrees of freedom), has become the preferred solution for such problems; see, e.g., [1–4] and the references cited therein. However, an important fact is that the lowest-order velocity-pressure pairs violate the LBB [5] (inf-sup) stability condition, which often leads to unphysical pressure oscillations. To overcome this difficulty, a series of methods have been developed, such as penalty methods [6–8], consistently stabilized methods [9, 10], pressure gradient projection methods [11–13], related local pressure gradient stabilization methods [14], offset pressure stabilization methods [15], and projection-based stabilized methods [16, 17], among others.

As an extension of the classical finite elements to general polygonal elements, the virtual element method (VEM) has gained widespread attention since its theory [18] and matrix implementation [19] were proposed. Then the authors in [20] enhanced a discrete space and gave a specific process in calculating an L^2-projection operator for a three-dimensional reaction-diffusion problem. By combing the ideas of VEM with other methods, the H^α-conforming VEM [21, 22], the nonconforming VEM [23, 24], and the $H(\mathrm{div})/H(\mathrm{curl})$-VEM [25, 26] were designed. Due to the advantages of the virtual element method in mesh flexibility and structure-preserving spatial construction, the VEM has been widely used in adaptive mesh refinement [27], elliptic bulk-surface PDEs [28], structural mechanics elasticity [29, 30] and incompressible fluid problems [31–36].

Combining the widespread practical applications of the lowest-order elements with the advantages of the virtual element method, it is crucial to construct the lowest-order virtual element pair, which, in fact, not only faces a similar situation to the lowest-order mixed finite elements (that is, the pair fails to satisfy the inf-sup stability condition), but also needs to consider the computability of additional stabilization terms introduced to meet this stability condition (since the VEM lacks explicit expressions of basis functions). About these challenges, the authors in [37] have developed the 'equal-order' stabilized virtual element pairs for the Stokes problem on polygonal meshes, utilizing a projection-based stabilization to circumvent the discrete inf-sup condition. In addition, the authors in [38] have proposed a least-squares type stabilization VEM for the Stokes problem, which is suitable for arbitrary combinations of velocity and pressure. Also, there is some research on stabilized virtual element methods for other problems, such as the Navier-Stokes [39], Oseen [40], advection-diffusion-reaction [41–43] problems, among others. Furthermore, it is worth mentioning that [31] has also provided a lowest-order virtual element pair (which amazingly satisfies the divergence-free property) for the Stokes problem by constructing a new virtual element space (rather than by adding a stabilization term), but which requires, in addition to point values at vertices, the point values of normal components at the midpoints of edges as degrees of freedom for velocity. Also, [31] also uses the stream formulation of the Stokes problem that naturally leads to a symmetric system.

This paper mainly focuses on constructing the lowest-order (i.e., a piecewise constant approximation for pressure and an approximation with an accuracy order $k=1$ for velocity) stabilized virtual elements for the two- and three-dimensional Stokes problems, which are different from the existing articles on virtual element stabilization. Based on the local pressure jump stabilization and the local pressure projection stabilization, we not only prove the two corresponding weaker forms of the inf-sup condition, which leads to the existence and uniqueness of the discrete solution, but also obtain the optimal H^1-error estimate for the velocity and the optimal L^2-error estimates for the velocity and pressure. Furthermore, we show the simple and straightforward matrix implementation of the discrete problem, including the local operators, the local stabilization term, and the suitable projection in the stabilization term. Importantly, our proposed scheme is a symmetric linear system that involves neither the calculations of higher-order derivatives nor additional coupling terms, and can deal with polygonal meshes (including non-convex and degenerate elements). Especially, our scheme is still parameter-free for the local pressure projection stabilization. Our numerical experiments in two and three dimensions are shown to confirm the theoretical predictions.

The layout of this paper is as follows: Section 2 presents the stabilized virtual element discretization. Section 3 gives the well-posedness of our discrete scheme. The corresponding error estimates are provided in Section 4, while some details of the matrix implementation are shown in Section 5. The paper concludes with Section 6 in which the results of a series of numerical experiments are demonstrated.

Throughout the paper, we use the standard notation of the Sobolev spaces, such as the Sobolev space $H^m(\mathcal{D})$ (when $m=0$, $H^0(\mathcal{D})$ represents $L^2(\mathcal{D})$) on an open bounded domain $\mathcal{D}$ and the corresponding inner product $(\cdot,\cdot)_{m,\mathcal{D}}$, norm $\|\cdot\|_{m,\mathcal{D}}$, and seminorm $|\cdot|_{m,\mathcal{D}}$. When $\mathcal{D}=\Omega$, we shall omit index Ω from the subscript for the inner products, norms and seminorms. Moreover, $\mathbb{P}_\ell(\mathcal{D})$ is defined as the set of polynomials of degree less than or equal to ℓ on $\mathcal{D}$; especially, $\mathbb{P}_{-1}(\mathcal{D})=\{0\}$.

2 Stabilized virtual element approximation

This section considers a stabilized virtual element approximation of the Stokes problem in an open and bounded polygonal/polyhedral domain $\Omega\subset\mathbb{R}^d$ $(d=2,3)$:

$$-\nu\Delta\mathbf{u}+\nabla p=\mathbf{f} \quad \text{in } \Omega, \tag{2.1a}$$
$$\nabla\cdot\mathbf{u}=0 \quad \text{in } \Omega, \tag{2.1b}$$
$$\mathbf{u}=\mathbf{0} \quad \text{on } \partial\Omega, \tag{2.1c}$$

with the unknown velocity $\mathbf{u}\in[H^2(\Omega)]^d$, the unknown pressure $p\in H^1(\Omega)$, the given viscosity ν, and the given external force $\mathbf{f}\in[L^2(\Omega)]^d$. Then, the weak formulation of problem (2.1) reads as: Find $(\mathbf{u},p)\in\mathbf{X}\times Z=[H_0^1(\Omega)]^d\times L_0^2(\Omega)$ such that, for all $\mathbf{v}\in\mathbf{X}$ and $q\in Z$,

$$\nu a(\mathbf{u},\mathbf{v})+b(\mathbf{v},p)=(\mathbf{f},\mathbf{v}), \tag{2.2a}$$
$$b(\mathbf{u},q)=0, \tag{2.2b}$$

or

$$\mathcal{A}(\mathbf{u},p;\mathbf{v},q)=(\mathbf{f},\mathbf{v}), \tag{2.3}$$

where $H_0^1(\Omega)$ denotes the space of $H^1(\Omega)$ functions with vanishing trace on the boundary, $L_0^2(\Omega)$ denotes the set of square integrable functions with a vanishing mean, and

$$a(\mathbf{u},\mathbf{v})=(\nabla\mathbf{u},\nabla\mathbf{v}), \quad b(\mathbf{v},p)=-(p,\nabla\cdot\mathbf{v}),$$
$$\mathcal{A}(\mathbf{u},p;\mathbf{v},q)=\nu a(\mathbf{u},\mathbf{v})+b(\mathbf{v},p)-b(\mathbf{u},q).$$

Obviously, the well-posedness of problem (2.2) (c.f. [44–46]) classically hinges on the continuity and coercivity of the bilinear form $a(\mathbf{u},\mathbf{v})$ on $\mathbf{X}\times\mathbf{X}$; i.e.,

$$|a(\mathbf{u},\mathbf{v})|\le C\|\mathbf{u}\|_1\|\mathbf{v}\|_1 \quad \text{and} \quad a(\mathbf{v},\mathbf{v})\ge C\|\mathbf{v}\|_1^2,$$

together with the continuity and inf-sup stability of the bilinear form $b(\mathbf{v},p)$ on $\mathbf{X}\times Z$, i.e.,

$$|b(\mathbf{v},p)|\le C\|p\|_0\|\mathbf{v}\|_1 \quad \text{and} \quad \sup_{\mathbf{v}\in\mathbf{X}}\frac{b(\mathbf{v},p)}{\|\mathbf{v}\|_1}\ge C\|p\|_0.$$

Here and below, we denote a generic positive constant C independent of a mesh size, which is different from place to place (unless otherwise stated).

2.1 Virtual element discrete spaces

In the two-dimensional case, let $\mathcal{T}_h$ be a decomposition of Ω into polygonal elements K with the maximum element size $h=\max\limits_{K\in\mathcal{T}_h}\mathrm{diam}(K)$. Then, all edges and vertices in $\mathcal{T}_h$ are collected in the sets $\mathcal{E}_h$ and $\mathcal{V}_h$, respectively. And the set of all edges of element K is defined as $\mathcal{E}(K)$. If we set $h_{\mathfrak{O}}=\mathrm{diam}(\mathfrak{O})$ with $\mathfrak{O}$ being selected as every polygonal element K or every edge e, the mesh partition is assumed to be shape-regular in the following sense:

Assumption 0 ([18])**.** We assume that for every h, decomposition $\mathcal{T}_h$ is made of a finite number of simple polygons, and there exists a positive real number γ such that the following properties hold: i) for every polygonal element K and edge $e\in\mathcal{E}(K)$, $h_e\geq\gamma h_K$; ii) every polygonal element K is star-shaped with respect to a disk of radius $\geq\gamma h_K$.

Now, for any two-dimensional polygonal element $K\in\mathcal{T}_h$ with n_e edges and $n_v=n_e$ vertices, we can define the lowest-order enhanced local discrete space for the velocity as

$$\begin{aligned}\mathbf{X}_{h|K}=\{\mathbf{v}_h\in[H^1(K)]^2:\ \Delta\mathbf{v}_h\in[\mathbb{P}_1(K)]^2,\ \mathbf{v}_h|_{\partial K}\in C^0(\partial K),\ \mathbf{v}_h|_e\in[\mathbb{P}_1(e)]^2 \text{ for each } e\in\mathcal{E}(K),\\ (\mathbf{v}_h-\Pi_K^{\nabla}\mathbf{v}_h,\mathbf{m})_K=0\ \ \forall\ \mathbf{m}\in[\mathbb{P}_1(K)]^2\},\end{aligned}$$

where the local H^1-projection $\Pi_K^{\nabla}:[H^1(K)]^d\rightarrow[\mathbb{P}_1(K)]^d$ is computable [20] and defined as

$$\begin{aligned}&(\nabla\Pi_K^{\nabla}\mathbf{v},\nabla\mathbf{m})_K=(\nabla\mathbf{v},\nabla\mathbf{m})_K\quad\forall\ \mathbf{m}\in[\mathbb{P}_1(K)]^d,\\ &(\Pi_K^{\nabla}\mathbf{v},1)_{\partial K}=(\mathbf{v},1)_{\partial K}.\end{aligned}\tag{2.4}$$

According to [20], we can introduce the values of $\mathbf{v}_h$ at the vertices in K as the unisolvent degrees of freedom, which coincide with the dimension of $\mathbf{X}_{h|K}$. Meanwhile, we can introduce the local L^2-orthogonal projection operators $\Pi_K^0:[L^2(K)]^d\rightarrow[\mathbb{P}_1(K)]^d$ and $\Pi_K^{00}\mathrm{div}:[H^1(K)]^d\rightarrow\mathbb{P}_0(K)$

$$\begin{aligned}(\Pi_K^0\mathbf{v},\mathbf{m})_K&=(\mathbf{v},\mathbf{m})_K\quad\forall\ \mathbf{m}\in[\mathbb{P}_1(K)]^d,\\ (\Pi_K^{00}\mathrm{div}\mathbf{v},m)_K&=(\mathrm{div}\mathbf{v},m)_K\quad\forall\ m\in\mathbb{P}_0(K),\end{aligned}\tag{2.5}$$

and ensure their computability from the degrees of freedom of $\mathbf{X}_{h|K}$ (a discussion on the computability of Π_K^0 and $\Pi_K^{00}\mathrm{div}$ is found in Remark 2.1 below).

In the three-dimensional case, we can similarly define the mesh partition $\mathcal{T}_h$ and additionally introduce all faces set $\mathcal{F}_h$, element faces set $\mathcal{F}(P)$ and the element size h_P for every polyhedron. Then, the regularity requirement of mesh partitions also requires two following conditions in addition to Assumption 0: i) for every polyhedral element P and face $K\in\mathcal{F}(P)$, $h_K\geq\gamma h_P$ with γ being the positive real number present in Assumption 0; ii) every polyhedral element P is star-shaped with respect to a sphere of radius $\geq\gamma h_P$. Now, the local space on every polyhedral element $P\in\mathcal{T}_h$ (with n_v vertices, n_K faces, and n_e edges) is defined by

$$\begin{aligned}\mathbf{X}_{h|P}=\{\mathbf{v}_h\in[H^1(P)]^3:\ \Delta\mathbf{v}_h\in[\mathbb{P}_1(P)]^3,\ \mathbf{v}_h|_{\partial P}\in H^1(\partial P),\ \mathbf{v}_h|_K\in\mathbf{X}_{h|K} \text{ for each } K\in\mathcal{F}(P)\\ (\mathbf{v}_h-\Pi_P^{\nabla}\mathbf{v}_h,\mathbf{m})_P=0\ \ \forall\ \mathbf{m}\in[\mathbb{P}_1(P)]^3\},\end{aligned}$$

which can be endowed with the unisolvent degrees of freedom, i.e., the values at the vertices of P.

To simplify the notation, in what follows we will use the unified symbol E to represent a two-dimensional polygonal element K or a three-dimensional polyhedral element P.

Now, whether the dimension d is 2 or 3, we can define the global virtual element space $\mathbf{X}_h$ for the velocity as a continuous space; i.e.,

$$\mathbf{X}_h=\{\mathbf{v}_h\in\mathbf{X}:\ \mathbf{v}_{h|E}\in\mathbf{X}_{h|E}\text{ for each }E\in\mathcal{T}_h\},$$

whose unisolvent degrees of freedom are chosen as the values of $\mathbf{v}_h$ at the internal vertices (remembering that on $\partial\Omega$ we set the homogeneous Dirichlet boundary conditions) of the decomposition. Immediately, the global discrete space for the pressure can be shown as a piecewise constant space; i.e.,

$$Z_h=\{q_h\in Z:\ q_{h|E}\in\mathbb{P}_0(E)\text{ for each }E\in\mathcal{T}_h\}.$$

Remark 2.1. It is obvious that these three projections Π_E^∇,Π_E^0, and $\Pi_E^{00}\mathrm{div}$ can be computed based on the degrees of freedom of the local discrete virtual element space $\mathbf{X}_{h|E}$. More specifically, the right-hand terms of these three projections can be expressed by the partial integral formula as

$$\begin{aligned}(\nabla\mathbf{v},\nabla\mathbf{m})_E&=(\mathbf{v},\nabla\mathbf{m}\cdot\mathbf{n}_E)_{\partial E}\quad\forall\,\mathbf{m}\in[\mathbb{P}_1(E)]^d,\\(\mathbf{v},\mathbf{m})_E&=(\Pi_E^\nabla\mathbf{v},\mathbf{m})_E\quad\forall\,\mathbf{m}\in[\mathbb{P}_1(E)]^d,\\(\mathrm{div}\mathbf{v},m)_E&=(\mathbf{v}\cdot\mathbf{n}_E,m)_{\partial E}\quad\forall\,m\in\mathbb{P}_0(E),\end{aligned}$$

with $\mathbf{n}_E$ being the exterior unit normal vector of element E. Since $\nabla\mathbf{m}\cdot\mathbf{n}_E\in\mathbb{P}_0(E)$ and $m\in\mathbb{P}_0(E)$, we can obtain the computability of the H^1-projection Π_E^∇ and composite projection $\Pi_E^{00}\mathrm{div}$, which leads to the computability of the L^2-projection Π_E^0. For more details, the reader is referred to [19].

2.2 Virtual element discrete schemes

From now on, we only need to discuss how to construct the discrete versions of the local bilinear forms $a^E(\cdot,\cdot),b^E(\cdot,\cdot)$ and the right-hand term, which lead to the global virtual element discrete schemes by simply summing the local contributions. If we number the degrees of freedom of the local space $\mathbf{X}_{h|E}$ from 1 to $N_E^{\mathrm{dof}}=\dim\mathbf{X}_{h|E}$ and we define the operator dof_i from $\mathbf{X}_{h|E}$ to $\mathbb{R}$ as

$$\mathrm{dof}_i(\mathbf{v}_h):=i\text{-th degree of freedom of }\mathbf{v}_h,\quad i=1,\cdots,N_E^{\mathrm{dof}},$$

the discrete counterpart of the bilinear form $a^E(\cdot,\cdot)$ can be defined as

$$a_h^E(\mathbf{u}_h,\mathbf{v}_h)=a^E(\Pi_E^\nabla\mathbf{u}_h,\Pi_E^\nabla\mathbf{v}_h)_K+S^E(\mathbf{u}_h-\Pi_E^\nabla\mathbf{u}_h,\mathbf{v}_h-\Pi_E^\nabla\mathbf{v}_h),\quad\mathbf{u}_h,\mathbf{v}_h\in\mathbf{X}_{h|E},\tag{2.6}$$

as proposed in [18,20], where the symmetric and positive definite bilinear form $S^E:\mathbf{X}_{h|E}\times\mathbf{X}_{h|E}\to\mathbb{R}$ guarantees

$$c_*a^E(\mathbf{v}_h,\mathbf{v}_h)\le S^E(\mathbf{v}_h,\mathbf{v}_h)\le c^*a^E(\mathbf{v}_h,\mathbf{v}_h)\quad\forall\,\mathbf{v}_h\in\ker(\Pi_E^\nabla),$$

for some positive constants c_* and c^* independent of h. A simple choice for $S^E(\cdot,\cdot)$ is the Euclidean inner product between vectors of degrees of freedom (other possible choices can be found in [47]); i.e.,

$$S^E(\mathbf{u}_h-\Pi_E^\nabla\mathbf{u}_h,\mathbf{v}_h-\Pi_E^\nabla\mathbf{v}_h)=h_E^{d-2}\sum_{i=1}^{N_E^{\mathrm{dof}}}\mathrm{dof}_i(\mathbf{u}_h-\Pi_E^\nabla\mathbf{u}_h)\mathrm{dof}_i(\mathbf{v}_h-\Pi_E^\nabla\mathbf{v}_h). \tag{2.7}$$

Thanks to the definition of operator Π_E^∇ and the continuity and coercivity of term $S^E(\cdot,\cdot)$, we can prove the crucial properties of the local discrete bilinear form $a_h^E(\cdot,\cdot)$:

i) k-consistency: for all $\mathbf{m}\in[\mathbb{P}_k(E)]^d$ and for all $\mathbf{v}_h\in\mathbf{X}_{h|E}$, it holds

$$a_h^E(\mathbf{v}_h,\mathbf{m})=a^E(\mathbf{v}_h,\mathbf{m});$$

ii) Stability: there exist two positive constants α_*,α^* independent of h, such that

$$\alpha_*\|\nabla\mathbf{v}_h\|_{0,E}^2\le a_h^E(\mathbf{v}_h,\mathbf{v}_h)\le\alpha^*\|\nabla\mathbf{v}_h\|_{0,E}^2\quad\forall\mathbf{v}_h\in\mathbf{X}_{h|E}.$$

At the same time, the local virtual element approximations of $b^E(\cdot,\cdot)$ and the local load term are, respectively, defined as

$$\begin{aligned}b_h^E(\mathbf{v}_h,p_h)&=-(\Pi_E^{00}\mathrm{div}\mathbf{v}_h,p_h)_E=-(\mathrm{div}\mathbf{v}_h,p_h)_E\quad\forall\mathbf{v}_h\in\mathbf{X}_{h|E},\ \ p_h\in Z_{h|E},\\(\mathbf{f}_h,\mathbf{v}_h)_E&=(\mathbf{f},\Pi_E^0\mathbf{v}_h)_E=(\Pi_E^0\mathbf{f},\mathbf{v}_h)_E\quad\forall\mathbf{v}_h\in\mathbf{X}_{h|E}.\end{aligned}\tag{2.8}$$

Next, due to the fact that lowest-order virtual element pairs $\mathbf{X}_h$ and Z_h violate the discrete inf-sup condition, a stabilization term has to be designed based on the pressure jump or the pressure projection. Following the ideas of [48], we can define a stabilization term for every $p_h,q_h\in Z_h$

$$G_1(p_h,q_h)=\delta\sum_{e\in\Gamma_h^0}\int_e h_e[[p_h]][[q_h]]\,ds, \tag{2.9}$$

where h_e denotes the size of an element edge ($d=2$) or face ($d=3$), Γ_h^0 indicates the set of all interior edges/faces in $\mathcal{T}_h$, $[[\cdot]]$ is the jump across an edge/face (taken on the interior edges/faces only), and δ represents a stabilization parameter that is independent of h (but its most appropriate choice is not known a priori). It is clear that this stabilization term is computable from degrees of freedom of Z_h and is related to the stabilization parameter δ. Then, if we define a norm

$$\|q\|_{\Gamma_h^0}=\left(\sum_{e\in\Gamma_h^0}\int_e q^2ds\right)^{\frac{1}{2}},$$

we can obtain the continuity and coercivity of $G_1(\cdot,\cdot)$, i.e.,

$$G_1(q_h,q_h)\ge\gamma_*\min_{e\in\Gamma_h^0}(h_e)\|[[q_h]]\|_{\Gamma_h^0}^2\quad\text{and}\quad G_1(p_h,q_h)\le\gamma^*\|p_h\|_0\|q_h\|_0 \tag{2.10}$$

by using the standard inverse inequality $\|[[p_h]]\|_{\Gamma_h^0} \leq Ch^{-1/2}\|p_h\|_0$ for all functions $p_h \in Z_h$ [49].

Furthermore, in order to design a parameter-free stabilization term, we should consider the following pressure projection scheme similar to [17]

$$\int_\Omega (p_h - \Pi p_h)(q_h - \Pi q_h)\, d\mathbf{x} = \int_\Omega p_h q_h - p_h \Pi q_h - q_h \Pi p_h + \Pi p_h \Pi q_h \, d\mathbf{x} \quad \forall p_h, q_h \in Z_h|_K,$$

where the interpolation operator $\Pi : L^2(\Omega) \to X_h$ (whose possible choices will be shown in Section 5) satisfies the continuity hypothesis (as an operator $L^2(\Omega) \to L^2(\Omega)$)

$$\|\Pi q\|_0 \leq C\|q\|_0 \tag{2.11}$$

and the approximation hypothesis

$$\|q - \Pi q\|_0 \leq Ch\|q\|_1, \tag{2.12}$$

where X_h is the scalar VEM space defined as

$$\begin{aligned} X_h = \{ v \in H^1(\Omega) : \ & \Delta v|_E \in \mathbb{P}_1(E) \ \ \forall E \in \mathcal{T}_h, \ v|_e \in \mathbb{P}_1(e) \ \ \forall e \in \mathcal{E}_h, \\ & (v - \Pi_E^\nabla v, m)_E = 0 \ \ \forall\, m \in \mathbb{P}_1(E),\ E \in \mathcal{T}_h \} \end{aligned}$$

for $d=2$ and as

$$\begin{aligned} X_h = \{ v \in H^1(\Omega) : \ & \Delta v|_E \in \mathbb{P}_1(E) \ \ \forall E \in \mathcal{T}_h,\ \Delta v|_F \in \mathbb{P}_1(F) \ \ \forall F \in \mathcal{F}_h,\ v|_e \in \mathbb{P}_1(e) \ \ \forall e \in \mathcal{E}_h, \\ & (v - \Pi_F^\nabla v, m)_F = 0 \ \ \forall\, m \in \mathbb{P}_1(F), \ \ (v - \Pi_E^\nabla v, m)_E = 0 \ \ \forall\, m \in \mathbb{P}_1(E) \} \end{aligned}$$

for $d=3$. Obviously, it holds that $\mathbf{X}_h = [X_h]^d$. Also, we can similarly introduce the spatial dimension $\widetilde{N}_E^{\text{dof}} = \dim X_{h|E} = N_E^{\text{dof}}/d$ and the i-th degree of freedom $\widetilde{\text{dof}}_i$ for the scalar space X_h.

However, it is unfortunate that the stabilization term designed above, essentially the term $\int_\Omega \Pi p_h \Pi q_h \, d\mathbf{x}$, is not computable in the framework of virtual element method, so we need to replace it with the following computable stabilization term:

$$\begin{aligned} G_2(p_h, q_h) = \sum_{E \in \mathcal{T}_h} \Big[& (p_h, q_h)_E - (p_h, \Pi q_h)_E - (\Pi p_h, q_h)_E \\ & + (\Pi_E^0 \Pi p_h, \Pi_E^0 \Pi q_h)_E + \widetilde{S}^E((I - \Pi_E^0)\Pi p_h, (I - \Pi_E^0)\Pi q_h) \Big], \end{aligned} \tag{2.13}$$

where the symmetric and positive definite bilinear form $\tilde{S}^E : X_{h|E} \times X_{h|E} \to \mathbb{R}$ can be simply defined as

$$\widetilde{S}^E((I - \Pi_E^0)\Pi p_h, (I - \Pi_E^0)\Pi q_h) = |E| \sum_{i=1}^{\widetilde{N}_E^{\text{dof}}} \widetilde{\text{dof}}_i((I - \Pi_E^0)\Pi p_h)\widetilde{\text{dof}}_i((I - \Pi_E^0)\Pi q_h). \tag{2.14}$$

It can be seen from [50] that

$$\begin{aligned}\widetilde{c}_*((I-\Pi_E^0)\Pi p_h,(I-\Pi_E^0)\Pi p_h)_E \le \widetilde{S}^E((I-\Pi_E^0)\Pi p_h,(I-\Pi_E^0)\Pi p_h)\\ \le \widetilde{c}^*((I-\Pi_E^0)\Pi p_h,(I-\Pi_E^0)\Pi p_h)_E\end{aligned}$$

for some positive constants $\widetilde{c}_*$ and $\widetilde{c}^*$ independent of h. Then, we know the continuity and coercivity of $G_2(\cdot,\cdot)$, i.e.,

$$G_2(q_h,q_h)\ge\gamma_*\|q_h-\Pi q_h\|_0^2 \quad \text{and} \quad G_2(p_h,q_h)\le\gamma^*\|p_h-\Pi p_h\|_0\|q_h-\Pi q_h\|_0. \tag{2.15}$$

In the end, we show the stabilized virtual element scheme for the Stokes problem: Find $(\mathbf{u}_h,p_h)\in\mathbf{X}_h\times Z_h$ such that

$$\nu a_h(\mathbf{u}_h,\mathbf{v}_h)+b_h(\mathbf{v}_h,p_h)=(\mathbf{f}_h,\mathbf{v}_h) \quad \forall\, \mathbf{v}_h\in\mathbf{X}_h, \tag{2.16a}$$
$$b_h(\mathbf{u}_h,q_h)-G(p_h,q_h)=0 \quad \forall\, q_h\in Z_h, \tag{2.16b}$$

where the stabilization term $G(\cdot,\cdot)$ is either $G_1(\cdot,\cdot)$ or $G_2(\cdot,\cdot)$. Equivalently, we can write (2.16) in the following form: Find $(\mathbf{u}_h,p_h)\in\mathbf{X}_h\times Z_h$ such that

$$\mathcal{A}_h(\mathbf{u}_h,p_h;\mathbf{v}_h,q_h)=(\mathbf{f}_h,\mathbf{v}_h) \quad \forall\, (\mathbf{v}_h,q_h)\in\mathbf{X}_h\times Z_h, \tag{2.17}$$

where

$$\mathcal{A}_h(\mathbf{u}_h,p_h;\mathbf{v}_h,q_h)=\nu a_h(\mathbf{u}_h,\mathbf{v}_h)+b_h(\mathbf{v}_h,p_h)-b_h(\mathbf{u}_h,q_h)+G(p_h,q_h).$$

Remark 2.2. When E is a triangle ($d=2$) or tetrahedron ($d=3$), the proposed stabilized virtual element method is the finite element case in [17], except for an approximation of the load term.

3 Well-posedness of the Discrete scheme

This section is devoted to recall the projection and interpolation errors, and prove the well-posedness of (2.17).

Lemma 3.1 ([51]). *If Assumption 0 is satisfied, then for every $E\in\mathcal{T}_h$ and $\mathbf{v}\in[H^{s+1}(K)]^d$, it holds that*

$$\|\mathbf{v}-\Pi_E^\nabla\mathbf{v}\|_{m,E}\le Ch_E^{s+1-m}\|\mathbf{v}\|_{s+1,E}, \quad m\in\mathbb{N},\ \max(m-1,0)\le s\le k,$$
$$\|\mathbf{v}-\Pi_E^0\mathbf{v}\|_{m,E}\le Ch_E^{s+1-m}\|\mathbf{v}\|_{s+1,E}, \quad m\in\mathbb{N},\ m-1\le s\le k.$$

Lemma 3.2 ([27,52]). *If Assumption 0 is satisfied, then for every $E\in\mathcal{T}_h$ and $\mathbf{v}\in[H^{s+1}(E)]^d$, there exist $\mathbf{v}_\pi\in\mathbb{P}_k(E)$ and $\mathbf{v}_I\in\mathbf{X}_{h|E}$ satisfying $dof_i(\mathbf{v}-\mathbf{v}_I)=0,i=1,\cdots,N_E^{dof}$ such that*

$$\|\mathbf{v}-\mathbf{v}_\pi\|_{0,E}+h_E|\mathbf{v}-\mathbf{v}_\pi|_{1,E}\le Ch_E^{s+1}|\mathbf{v}|_{s+1,E}, \quad 0\le s\le k,$$
$$\|\mathbf{v}-\mathbf{v}_I\|_{0,E}+h_E|\mathbf{v}-\mathbf{v}_I|_{1,E}\le Ch_E^{s+1}|\mathbf{v}|_{s+1,E}, \quad 1\le s\le k.$$

Lemma 3.3 ([27, 52]). *If Assumption 0 is satisfied and $\widetilde{E}$ is a partition of E into triangles or tetrahedra, then for every $E\in\mathcal{T}_h$ and $\mathbf{v}\in[H^1(\Omega)]^d$, there exists $\mathbf{v}_c\in\mathbf{X}_h$ such that*

$$\|\mathbf{v}-\mathbf{v}_c\|_{0,E}+h_E|\mathbf{v}-\mathbf{v}_c|_{1,E}\leq C(\gamma)h_E|\mathbf{v}|_{1,\widetilde{E}}.$$

To show that (2.17) is a stable variational problem, we have to show that $\mathcal{A}_h$ is continuous, i.e., that there exists $C>0$ such that for all $(\mathbf{u}_h,p_h)$ and $(\mathbf{v}_h,q_h)$ in $\mathbf{X}_h\times Z_h$, it holds that

$$\mathcal{A}_h(\mathbf{u}_h,p_h;\mathbf{v}_h,q_h)\leq C(\|\mathbf{u}_h\|_1+\|p_h\|_0)(\|\mathbf{v}_h\|_1+\|q_h\|_0), \tag{3.1}$$

where the hypothesis (2.11) is used for the case $G(\cdot,\cdot)=G_2(\cdot,\cdot)$. Then, we need to prove two weaker forms of the inf-sup condition corresponding to $G_1(\cdot,\cdot)$ and $G_2(\cdot,\cdot)$.

Lemma 3.4. *If Assumption 0 is satisfied, there exist positive constants β_1 and $\widehat{\beta}_1$ independent of h such that*

$$\sup_{\mathbf{v}_h\in\mathbf{X}_h}\frac{|(\nabla\cdot\mathbf{v}_h,q_h)|}{\|\mathbf{v}_h\|_1}\geq\beta_1\|q_h\|_0-\widehat{\beta}_1h^{1/2}\|[[q_h]]\|_{\Gamma_h^0}\quad\forall\, q_h\in Z_h.$$

Proof. Due to the fact that $q_h\in Z_h\subset Z$, there exists $\mathbf{w}\in[H_0^1(\Omega)]^d$ such that

$$\left|\int_\Omega q_h\nabla\cdot\mathbf{w}d\mathbf{x}\right|\geq C_1\|q_h\|_0\|\mathbf{w}\|_1.$$

Then, from Lemma 3.3, it is known that there exists a $\mathbf{w}_c\in\mathbf{X}_h\subset[H_0^1(\Omega)]^d$ satisfying $\|\mathbf{w}_c\|_1\leq C_2\|\mathbf{w}\|_1$, which leads to

$$\frac{|(\nabla\cdot\mathbf{w}_c,q_h)|}{\|\mathbf{w}_c\|_1}\geq\frac{|(\nabla\cdot\mathbf{w}_c,q_h)|}{C_2\|\mathbf{w}\|_1}\geq\frac{C_1}{C_2}\|q_h\|_0-\frac{|(\nabla\cdot(\mathbf{w}-\mathbf{w}_c),q_h)|}{C_2\|\mathbf{w}\|_1}.$$

By using integrating by parts and the fact that q_h is constant on each element, we have

$$\begin{aligned}(\nabla\cdot(\mathbf{w}-\mathbf{w}_c),q_h)&=\sum_{E\in\mathcal{T}_h}\int_E\nabla\cdot(\mathbf{w}-\mathbf{w}_c)q_hd\mathbf{x}=\sum_{E\in\mathcal{T}_h}\int_{\partial E}\mathbf{n}_E\cdot(\mathbf{w}-\mathbf{w}_c)q_hds\\&=\sum_{e\in\Gamma_h^0}\int_e[[q_h]]\mathbf{n}_e\cdot(\mathbf{w}-\mathbf{w}_c)ds\leq C_3h^{1/2}\|[[q_h]]\|_{\Gamma_h^0}\|\mathbf{w}\|_1,\end{aligned}$$

where in the last step the Cauchy-Schwarz inequality, the trace inequality (c.f. (2.18) in [53]) and Lemma 3.3 are used. Now, since

$$\sup_{\mathbf{v}_h\in\mathbf{X}_h,\mathbf{v}_h\neq\mathbf{0}}\frac{|(\nabla\cdot\mathbf{v}_h,q_h)|}{\|\mathbf{v}_h\|_1}\geq\frac{|(\nabla\cdot\mathbf{w}_c,q_h)|}{\|\mathbf{w}_c\|_1},$$

the lemma is proved. $\square$

Lemma 3.5. *If Assumption* 0 *is satisfied, there exist positive constants* β_2 *and* $\widehat{\beta}_2$ *independent of* h *such that*

$$\sup_{\mathbf{v}_h\in\mathbf{X}_h}\frac{|(\nabla\cdot\mathbf{v}_h,q_h)|}{\|\mathbf{v}_h\|_1}\geq\beta_2\|q_h\|_0-\widehat{\beta}_2\|q_h-\Pi q_h\|_0\quad\forall\, q_h\in Z_h.$$

Proof. To prove this lemma, we only need to show $h^{1/2}\|[[q_h]]\|_{\Gamma_h^0}\leq C\|q_h-\Pi q_h\|_0$. From the definition of Π, it holds that $\Pi q_h\in C^0(\Omega)$ and $[[\Pi q_h|_e]]=0$ for every $e\in\Gamma_h^0$. Then, using the standard inverse inequality $\|[[p_h]]\|_{\Gamma_h^0}\leq Ch^{-1/2}\|p_h\|_0$, we have

$$h\|[[q_h]]\|^2_{\Gamma_h^0}=h\sum_{e\in\Gamma_h^0}\int_e([[q_h-\Pi q_h]]+[[\Pi q_h]])^2ds\leq C\|q_h-\Pi q_h\|_0^2,$$

which leads to the desired result. □

Now, the existence and uniqueness of the solution of (2.17) follow from the following lemma, together with (3.1):

Lemma 3.6. *If Assumption* 0 *is satisfied, it holds for each* $(\mathbf{u}_h,p_h)\in\mathbf{X}_h\times Z_h$

$$\sup_{(\mathbf{v}_h,q_h)\in\mathbf{X}_h\times Z_h}\frac{|\mathcal{A}_h(\mathbf{u}_h,p_h;\mathbf{v}_h,q_h)|}{\|\mathbf{v}_h\|_1+\|q_h\|_0}\geq C(\|\mathbf{u}_h\|_1+\|p_h\|_0).$$

Proof. For a given arbitrary but fixed pressure $p_h\in Z_h$, we can find $\mathbf{w}\in[H_0^1(\Omega)]^d$ satisfying $-\nabla\cdot\mathbf{w}=p_h,\|\mathbf{w}\|_1\leq C_4\|p_h\|_0$ and introduce a corresponding $\mathbf{w}_c$ from Lemma 3.4. Now, we can set $(\mathbf{v}_h,q_h)=(\mathbf{u}_h+\vartheta\mathbf{w}_c,p_h)$ with $\vartheta>0$ being a real parameter, which satisfies

$$\begin{aligned}\|\mathbf{v}_h\|_1+\|q_h\|_0&\leq\|\mathbf{u}_h\|_1+\vartheta\|\mathbf{w}_c\|_1+\|p_h\|_0\\&\leq\|\mathbf{u}_h\|_1+\vartheta C_2\|\mathbf{w}\|_1+\|p_h\|_0\leq C(\|\mathbf{u}_h\|_1+\|p_h\|_0).\end{aligned}\tag{3.2}$$

By using the equality $\|p_h\|_0^2+(p_h,\nabla\cdot\mathbf{w})=0$, the coercivity of $a_h(\cdot,\cdot)$ and the Young's inequality, we have the bound

$$\begin{aligned}&\mathcal{A}_h(\mathbf{u}_h,p_h;\mathbf{u}_h+\vartheta\mathbf{w}_c,p_h)\\&=\nu a_h(\mathbf{u}_h,\mathbf{u}_h)+\nu\vartheta a_h(\mathbf{u}_h,\mathbf{w}_c)+\vartheta b_h(\mathbf{w}_c,p_h)+G(p_h,p_h)+\vartheta\|p_h\|_0^2+\vartheta(p_h,\nabla\cdot\mathbf{w})\\&\geq\nu\alpha_*\|\mathbf{u}_h\|_1^2+\vartheta\|p_h\|_0^2+G(p_h,p_h)+\nu\vartheta a_h(\mathbf{u}_h,\mathbf{w}_c)+\vartheta(p_h,\nabla\cdot(\mathbf{w}-\mathbf{w}_c))\\&\geq\nu\alpha_*\left(1-\frac{\nu\vartheta\alpha^{*2}C_2^2C_4^2}{\alpha_*}\right)\|\mathbf{u}_h\|_1^2+\frac{\vartheta}{2}\|p_h\|_0^2+\left(1-\vartheta C_3^2C_4^2\right)G(p_h,p_h).\end{aligned}\tag{3.3}$$

Choosing

$$\vartheta=\min\left\{\frac{\alpha_*}{2\nu\alpha^{*2}C_2^2C_4^2},\frac{1}{2C_3^2C_4^2}\right\}$$

guarantees that

$$\left(1-\frac{\nu\vartheta\alpha^{*2}C_2^2C_4^2}{\alpha_*}\right)\geq\frac{1}{2}\quad\text{and}\quad\left(1-\vartheta C_3^2C_4^2\right)\geq\frac{1}{2},$$

which leads to

$$\begin{aligned}&\mathcal{A}_h(\mathbf{u}_h,p_h;\mathbf{u}_h+\vartheta\mathbf{w}_c,p_h)\\ \geq&\frac{1}{4}\left(\sqrt{\nu\alpha_*}\|\mathbf{u}_h\|_1+\sqrt{\vartheta}\|p_h\|_0\right)^2\\ \geq&C\left(\|\mathbf{u}_h\|_1+\|p_h\|_0\right)^2.\end{aligned}$$

Combing with (3.2), we get the desired discrete inf-sup condition. □

Remark 3.1. It is clear that the constant C in Lemma 3.6 (and subsequently in Theorems 4.1-4.2) is related to the viscosity parameter ν. If one wants to further ensure that the conforming discrete velocity can be exactly divergence-free, we can refer to the ideas in [54], which will be our future work.

4 Error estimates

The goal of this section is to achieve the H^1-error estimation for the velocity and the L^2-error estimation for the velocity and pressure.

Theorem 4.1. *Under the Assumption 0 for the family of meshes $\mathcal{T}_h$, let $(\mathbf{u},p)\in\{\mathbf{X}\cap[H^2(\Omega)]^d\}\times\{Z\cap H^1(\Omega)\}$ and $(\mathbf{u}_h,p_h)\in\mathbf{X}_h\times Z_h$ denote the solutions of* (2.2) *and* (2.16)*, respectively. Then, it holds*

$$\|\mathbf{u}-\mathbf{u}_h\|_1+\|p-p_h\|_0\leq Ch(\|\mathbf{u}\|_2+\|p\|_1+\|\mathbf{f}\|_1).$$

Proof. Taking $\mathbf{v}=\mathbf{v}_h\in\mathbf{X}_h$, $q=q_h\in Z_h$ in (2.3) and subtracting the obtained equation from (2.17), we can derive

$$\begin{aligned}&\nu(a(\mathbf{u},\mathbf{v}_h)-a_h(\mathbf{u}_h,\mathbf{v}_h))+(b(\mathbf{v}_h,p)-b_h(\mathbf{v}_h,p_h))\\&\qquad-(b(\mathbf{u},q_h)-b_h(\mathbf{u}_h,q_h))-G(p_h,q_h)=(\mathbf{f}-\mathbf{f}_h,\mathbf{v}_h),\end{aligned}\tag{4.1}$$

which leads to

$$\begin{aligned}\mathcal{A}_h(\mathbf{u}_h-\mathbf{u}_I,p_h-p_I;\mathbf{v}_h,q_h)=&\nu\sum_{E\in\mathcal{T}_h}\Big[a^E(\mathbf{u}-\mathbf{u}_\pi,\mathbf{v}_h)+a_h^E(\mathbf{u}_\pi-\mathbf{u},\mathbf{v}_h)+a_h^E(\mathbf{u}-\mathbf{u}_I,\mathbf{v}_h)\Big]\\&+b(\mathbf{v}_h,p-p_I)-b(\mathbf{u}-\mathbf{u}_I,q_h)+(\mathbf{f}_h-\mathbf{f},\mathbf{v}_h)-G(p_I,q_h).\end{aligned}\tag{4.2}$$

Obviously, by using Lemmas 3.1-3.2, the continuity and stability of the continuous and discrete bilinear forms, it holds

$$\begin{aligned}&a^E(\mathbf{u}-\mathbf{u}_\pi,\mathbf{v}_h)+a_h^E(\mathbf{u}_\pi-\mathbf{u},\mathbf{v}_h)+a_h^E(\mathbf{u}-\mathbf{u}_I,\mathbf{v}_h)\leq Ch\|\mathbf{u}\|_{2,E}\|\mathbf{v}_h\|_{1,E},\\&b(\mathbf{v}_h,p-p_I)+(\mathbf{f}_h-\mathbf{f},\mathbf{v}_h)\leq C\Big(\|p-p_I\|_0+\sum_{E\in\mathcal{T}_h}\|\mathbf{f}-\Pi_E^0\mathbf{f}\|_{0,E}\Big)\|\mathbf{v}_h\|_1\leq Ch(\|p\|_1+\|\mathbf{f}\|_1)\|\mathbf{v}_h\|_1,\\&-b(\mathbf{u}-\mathbf{u}_I,q_h)\leq C\|\mathbf{u}-\mathbf{u}_I\|_1\|q_h\|_0\leq Ch\|\mathbf{u}\|_2\|q_h\|_0.\end{aligned}\tag{4.3}$$

Also, according to the fact that $[[p|_e]]=0\ \forall e\in\Gamma_h^0$, the Cauchy-Schwarz inequality and the trace inequality (c.f. (2.18) in [53]), we have the following estimation for the local pressure jump stabilization $G(\cdot,\cdot)=G_1(\cdot,\cdot)$

$$\begin{aligned}|-G(p_I,q_h)|\leq&|G(p-p_I,q_h)|+\left|\sum_{e\in\Gamma_h^0}\int_e\delta h_e[[p]][[q_h]]\,ds\right|\\ \leq&C(\|p-p_I\|_0+h|p-p_I|_1)\|q_h\|_0\leq Ch\|p\|_1\|q_h\|_0,\end{aligned}\tag{4.4}$$

or get the following estimation from (2.11), (2.12), and (2.15) for the local pressure projection stabilization $G(\cdot,\cdot)=G_2(\cdot,\cdot)$

$$|-G(p_I,q_h)|\leq C(\|p_I-p\|_0+\|p-\Pi p\|_0+\|\Pi(p-p_I)\|_0)\|q_h-\Pi q_h\|_0\leq Ch\|p\|_1\|q_h\|_0.\tag{4.5}$$

It is immediate from Lemma 3.6, together with (4.3)-(4.5) to obtain

$$\|\mathbf{u}_h-\mathbf{u}_I\|_1+\|p_h-p_I\|_0\leq\frac{\mathcal{A}_h(\mathbf{u}_h-\mathbf{u}_I,p_h-p_I;\mathbf{v}_h,q_h)}{\|\mathbf{v}_h\|_1+\|q_h\|_0}\leq Ch(\|\mathbf{u}\|_2+\|p\|_1+\|\mathbf{f}\|_1).\tag{4.6}$$

Then, by applying the triangle inequality, we can get the desired result. □

In order to show the L^2-velocity error estimation, we need the following reasonable elliptic regularity assumption [44–46]: when the domain Ω is convex, there exists ρ depending only on Ω, such that for all $\mathbf{g}\in[L^2(\Omega)]^d$, the unique solution of the dual problem

$$-\nu\Delta\boldsymbol{\varpi}-\nabla\chi=\mathbf{g},\quad \text{in }\Omega,\tag{4.7a}$$
$$\operatorname{div}\boldsymbol{\varpi}=0,\quad \text{in }\Omega,\tag{4.7b}$$
$$\boldsymbol{\varpi}=\mathbf{0},\quad \text{on }\partial\Omega,\tag{4.7c}$$

satisfies the regularity estimate

$$\nu\|\boldsymbol{\varpi}\|_2+\|\chi\|_1\leq\rho\|\mathbf{g}\|_0.\tag{4.8}$$

Theorem 4.2. *Under the assumptions of Theorem* 4.1 *and the above elliptic regularity assumption, it holds*

$$\|\mathbf{u}-\mathbf{u}_h\|_0\leq Ch^2(\|\mathbf{u}\|_2+\|p\|_1+\|\mathbf{f}\|_1).$$

Proof. If we set $\mathbf{g}=\mathbf{u}-\mathbf{u}_h$ in (4.7), a direct calculation shows that

$$\begin{aligned}\|\mathbf{u}-\mathbf{u}_h\|_0^2=&(-\nu\Delta\boldsymbol{\varpi}-\nabla\chi,\mathbf{u}-\mathbf{u}_h)=\nu a(\boldsymbol{\varpi},\mathbf{u}-\mathbf{u}_h)-b(\mathbf{u}-\mathbf{u}_h,\chi)\\ =&\nu a(\boldsymbol{\varpi}-\boldsymbol{\varpi}_I,\mathbf{u}-\mathbf{u}_h)-b(\mathbf{u}-\mathbf{u}_h,\chi-\chi_I)+\nu a(\boldsymbol{\varpi}_I,\mathbf{u}-\mathbf{u}_h)-b(\mathbf{u}-\mathbf{u}_h,\chi_I).\end{aligned}\tag{4.9}$$

It is easy to obtain

$$
\begin{aligned}
\nu a(\boldsymbol{\varpi}-\boldsymbol{\varpi}_I,\mathbf{u}-\mathbf{u}_h)-b(\mathbf{u}-\mathbf{u}_h,\chi-\chi_I)&\le C(\nu\|\boldsymbol{\varpi}-\boldsymbol{\varpi}_I\|_1+\|\chi-\chi_I\|_0)\|\mathbf{u}-\mathbf{u}_h\|_1\\
&\le Ch\|\mathbf{u}-\mathbf{u}_h\|_0\|\mathbf{u}-\mathbf{u}_h\|_1.
\end{aligned}\tag{4.10}
$$

Now, the key is the estimation of the remainder $\nu a(\boldsymbol{\varpi}_I,\mathbf{u}-\mathbf{u}_h)-b(\mathbf{u}-\mathbf{u}_h,\chi_I)$, which can be rewritten as

$$
\begin{aligned}
\nu a(\boldsymbol{\varpi}_I,\mathbf{u}-\mathbf{u}_h)-b(\mathbf{u}-\mathbf{u}_h,\chi_I)=&-\nu\sum_{E\in\mathcal{T}_h}\Big[a^E(\mathbf{u}_h-\mathbf{u}_\pi,\boldsymbol{\varpi}_I-\boldsymbol{\varpi}_\pi)-a_h^E(\mathbf{u}_h-\mathbf{u}_\pi,\boldsymbol{\varpi}_I-\boldsymbol{\varpi}_\pi)\Big]\\
&+[(\mathbf{f}-\mathbf{f}_h,\boldsymbol{\varpi}_I)-b(\boldsymbol{\varpi}_I,p-p_h)]+G(p_h,\chi_I)
\end{aligned}\tag{4.11}
$$

by using (4.1) with $\mathbf{v}_h=\boldsymbol{\varpi}_I,q_h=\chi_I$, the k-consistency of $a_h^E(\cdot,\cdot)$, and the fact that $b(\mathbf{u}_h,\chi_I)=b_h(\mathbf{u}_h,\chi_I)$. Then, the first term of (4.11) can be estimated by adding or subtracting $\mathbf{u}$, i.e.,

$$
\begin{aligned}
&a^E(\mathbf{u}_h-\mathbf{u}_\pi,\boldsymbol{\varpi}_I-\boldsymbol{\varpi}_\pi)-a_h^E(\mathbf{u}_h-\mathbf{u}_\pi,\boldsymbol{\varpi}_I-\boldsymbol{\varpi}_\pi)\\
\le& C(\|\mathbf{u}-\mathbf{u}_h\|_1+\|\mathbf{u}-\mathbf{u}_\pi\|_1)(\|\boldsymbol{\varpi}_I-\boldsymbol{\varpi}\|_1+\|\boldsymbol{\varpi}-\boldsymbol{\varpi}_\pi\|_1)\\
\le& Ch(\|\mathbf{u}-\mathbf{u}_h\|_1+h\|\mathbf{u}\|_2)\|\mathbf{u}-\mathbf{u}_h\|_0.
\end{aligned}\tag{4.12}
$$

The second term of (4.11) can be estimated by the definition of Π_E^0 and the fact that $b(\boldsymbol{\varpi},p-p_h)=0$, i.e.,

$$
\begin{aligned}
(\mathbf{f}-\mathbf{f}_h,\boldsymbol{\varpi}_I)-b(\boldsymbol{\varpi}_I,p-p_h)&=\sum_{E\in\mathcal{T}_h}(\mathbf{f}-\Pi_E^0\mathbf{f},\boldsymbol{\varpi}_I-\Pi_E^0\boldsymbol{\varpi}_I)_E-b(\boldsymbol{\varpi}_I-\boldsymbol{\varpi},p-p_h)\\
&\le Ch(\|p-p_h\|_0+\sum_{E\in\mathcal{T}_h}\|\mathbf{f}-\Pi_E^0\mathbf{f}\|_{0,E})\|\boldsymbol{\varpi}\|_2\\
&\le Ch(\|p-p_h\|_0+h\|\mathbf{f}\|_1)\|\mathbf{u}-\mathbf{u}_h\|_0.
\end{aligned}\tag{4.13}
$$

The third term of (4.11) can be estimated by using the fact that $[[p|_e]]=0$ and $[[\chi|_e]]=0$ for all $e\in\Gamma_h^0$, and (2.11), (2.12), (2.15), i.e., for the case $G(\cdot,\cdot)=G_1(\cdot,\cdot)$, it holds that

$$
\begin{aligned}
G(p_h,\chi_I)&=G(p_h-p,\chi_I-\chi)+G(p,\chi_I)+G(p_h-p,\chi)\\
&\le C\|p_h-p\|_0\|\chi_I-\chi\|_0\le Ch\|p-p_h\|_0\|\mathbf{u}-\mathbf{u}_h\|_0,
\end{aligned}\tag{4.14}
$$

and for the case $G(\cdot,\cdot)=G_2(\cdot,\cdot)$, it holds that

$$
\begin{aligned}
G(p_h,\chi_I)&\le C(\|p_h-p\|_0+\|p-\Pi p\|_0+\|\Pi(p-p_h)\|_0)\|\chi_I-\Pi\chi_I\|_0\\
&\le Ch(\|p-p_h\|_0+h\|p\|_1)\|\mathbf{u}-\mathbf{u}_h\|_0.
\end{aligned}\tag{4.15}
$$

Therefore, substituting (4.10)-(4.15) into (4.9) and combining with Theorem 4.2, we end this proof. $\square$

5 Matrix implementation

In order to show the matrix expression for the VEM local stiffness matrix, we take the two-dimensional case as an example (the three-dimensional case can be obtained similarly) and first introduce two sets $\{\psi_i\}$ and $\{\varphi_i\}$ with cardinalities N_u and N_p as the basis functions of the virtual element spaces X_h and Z_h, respectively, which means the set

$$\left\{\begin{pmatrix}\psi_i\\0\end{pmatrix},\begin{pmatrix}0\\\psi_i\end{pmatrix}\right\}:=\boldsymbol{\phi}_j,\quad j=1,\cdots,2N_u$$

is a basis of the virtual element space $\mathbf{X}_h$. Then, we have three Lagrange-type interpolation identities:

$$\mathbf{u}_h=\begin{pmatrix}u_{1h}\\u_{2h}\end{pmatrix}=\begin{pmatrix}\sum\limits_{j=1}^{N_u}u_{1j}\psi_j\\\sum\limits_{j=1}^{N_u}u_{2j}\psi_j\end{pmatrix}=\sum_{j=1}^{2N_u}u_j\boldsymbol{\phi}_j\in\mathbf{X}_h,\quad v_h=\sum_{j=1}^{N_u}v_j\psi_j\in X_h,\quad p_h=\sum_{j=1}^{N_p}p_j\varphi_j\in Z_h, \tag{5.1}$$

where $u_j=u_{1j}$ for $j=1,\cdots,N_u$ and $u_j=u_{2j}$ for $j=N_u+1,\cdots,2N_u$. Also, we introduce the basis functions of $\mathbb{P}_k(E)$ as

$$m_1=1,\ m_2=\frac{x-x_E}{h_E},\ m_3=\frac{y-y_E}{h_E},\ m_4=\frac{(x-x_E)^2}{h_E^2},\ m_5=\frac{(x-x_E)(y-y_E)}{h_E^2},\ m_6=\frac{(y-y_E)^2}{h_E^2},\cdots,$$

i.e., $\{m_\lambda\}_{1\leq\lambda\leq n_k}$ with $n_k=\frac{(k+2)(k+1)}{2}$.

From the relationship between the scalar space X_h and the vector space $\mathbf{X}_h$, it is clear that we only need to guarantee the computability of the local operators Π_E^∇,Π_E^0 on the space X_h, which helps to achieve their computability on $\mathbf{X}_h$. More specifically, for the operator Π_E^∇, the linear system arising from its definition (2.4) can be written in the following matrix form:

$$G\begin{pmatrix}s_1^1 & s_2^1 & \cdots & s_{N_u}^1\\ s_1^2 & s_2^2 & \cdots & s_{N_u}^2\\ \vdots & \vdots & \ddots & \vdots\\ s_1^{n_k} & s_2^{n_k} & \cdots & s_{N_u}^{n_k}\end{pmatrix}=B,$$

where the elements in row 1, column j and row $i\in[2,n_k]$, column j of G are $(m_j,1)_{\partial E}$, $j=1,\cdots,n_k$ and $(\nabla m_j,\nabla m_i)_E$, $j=1,\cdots,n_k$, respectively; the elements in row 1, column j and row $i\in[2,n_k]$, column j of B are $(\psi_j,1)_{\partial E}$, $j=1,\cdots,N_u$ and $(\nabla\psi_j,\nabla m_i)_E$, $j=1,\cdots,N_u$, respectively; the coefficients of Π_E^∇ in the basis m_i, $i=1,\cdots,n_k$ are defined as s_j^i, $j=1,\cdots,N_u$, i.e.,

$$\Pi_E^\nabla\psi_j=\sum_{i=1}^{n_k}s_j^i m_i,\quad j=1,\cdots,N_u.$$

For the operator Π_E^0, the linear system arising from its definition (2.5) can be written in the following matrix form:

$$H\begin{pmatrix} t_1^1 & t_2^1 & \cdots & t_{N_u}^1 \\ t_1^2 & t_2^2 & \cdots & t_{N_u}^2 \\ \vdots & \vdots & \ddots & \vdots \\ t_1^{n_k} & t_2^{n_k} & \cdots & t_{N_u}^{n_k} \end{pmatrix} = C,$$

where the elements in the i-th row and j-th column of H are $(m_j,m_i)_E, i,j=1,\cdots,n_k$; C is the $n_k\times N_u$ matrix with $C_{ij}=(\psi_j,m_i)_E$ for $1\le i\le n_{k-2}$ and $C_{ij}=(\Pi_E^\nabla\psi_j,m_i)_E$ for $n_{k-2}+1\le i\le n_k$; the coefficients of Π_E^0 in the basis m_i, $i=1,\cdots,n_k$ are defined as t_j^i, $j=1,\cdots,N_u$, i.e.,

$$\Pi_E^0\psi_j=\sum_{i=1}^{n_k} t_j^i m_i, \quad j=1,\cdots,N_u.$$

Also, we can give the matrix $\widetilde{G}$ that coincides with G except for the first row which is set to zero and define the $N_u\times n_k$ matrix D by

$$D=\begin{pmatrix} \mathrm{dof}_1(m_1) & \mathrm{dof}_1(m_2) & \cdots & \mathrm{dof}_1(m_{n_k}) \\ \mathrm{dof}_2(m_1) & \mathrm{dof}_2(m_2) & \cdots & \mathrm{dof}_2(m_{n_k}) \\ \vdots & \vdots & \ddots & \vdots \\ \mathrm{dof}_{N_u}(m_1) & \mathrm{dof}_{N_u}(m_2) & \cdots & \mathrm{dof}_{N_u}(m_{n_k}) \end{pmatrix}.$$

In general, the matrix representations of the operators Π_E^∇ and Π_E^0 acting from $X_{h|E}$ to $\mathbb{P}_1(E)$ in the basis $\{m_\lambda\}$ are given by $G^{-1}B$ and $H^{-1}C$, respectively; Furthermore, we have the corresponding matrix representations

$$\mathbf{G}^{-1}\mathbf{B}:=\begin{pmatrix} G & 0 \\ 0 & G\end{pmatrix}^{-1}\begin{pmatrix} B & 0 \\ 0 & B\end{pmatrix} \quad \text{and} \quad \mathbf{H}^{-1}\mathbf{C}:=\begin{pmatrix} H & 0 \\ 0 & H\end{pmatrix}^{-1}\begin{pmatrix} C & 0 \\ 0 & C\end{pmatrix}$$

acting from $\mathbf{X}_{h|E}$ to $[\mathbb{P}_1(E)]^2$ in the basis $[\{m_\lambda\}]^2$. Meanwhile, proceeding as before, we define the $n_{k-1}\times n_{k-1}$ matrix

$$(H_{k-1})_{i,j}=(m_j,m_i)_E, \quad i,j=1,\cdots,n_{k-1}$$

and the $n_{k-1}\times 2N_u$ matrix

$$\begin{aligned}\mathbf{Q}_{i,j}&=(\mathrm{div}\boldsymbol{\phi}_j,m_i)_E, \quad i=1,\cdots,n_{k-1}, \ j=1,\cdots,2N_u\\ &=\left(\left(\frac{\partial\psi_j}{\partial x},m_i\right)_E \quad \left(\frac{\partial\psi_j}{\partial y},m_i\right)_E\right), \quad j=1,\cdots,N_u\end{aligned}$$

for the composition operator $\Pi_E^{00}\mathrm{div}$, which means that the coefficients of $\Pi_E^{00}\mathrm{div}\boldsymbol{\phi}_j$, $j=1,\cdots,2N_u$ in the basis m_i, $i=1,\cdots,n_{k-1}$ can be expressed as $(H_{k-1})^{-1}\mathbf{Q}$. Readers can refer to [19] for more details on matrix implementation of these operators.

Now, we can show the matrix expression for the VEM local stiffness matrix with the $2N_u \times 2N_u$ identity matrix $\mathbf{I}$, the matrix

$$\mathbf{D}=\begin{pmatrix} D & 0 \\ 0 & D \end{pmatrix}, \quad \widetilde{\mathbf{G}}=\begin{pmatrix} \widetilde{G} & 0 \\ 0 & \widetilde{G} \end{pmatrix},$$

and the $N_p \times N_p$ matrix $M_{i,j}=G(\varphi_j,\varphi_i)$ corresponding to the local pressure jump/projection stabilization

$$\begin{pmatrix} (\mathbf{G}^{-1}\mathbf{B})^T\widetilde{\mathbf{G}}(\mathbf{G}^{-1}\mathbf{B})+(\mathbf{I}-\mathbf{D}\mathbf{G}^{-1}\mathbf{B})^T(\mathbf{I}-\mathbf{D}\mathbf{G}^{-1}\mathbf{B}) & -((H_{k-1})^{-1}\mathbf{Q})^T \\ (H_{k-1})^{-1}\mathbf{Q} & M \end{pmatrix}. \tag{5.2}$$

Obviously, the key now becomes how to represent M, that is, the computability of the local pressure jump/projection stabilization term $G(\varphi_j,\varphi_i)$:

• For the case $G(\cdot,\cdot)=G_1(\cdot,\cdot)$, its computability can be easily obtained from the definition of the jump operator $[[\cdot]]$ and the fact that $\varphi_j \in Z_h$ (be a piecewise constant);

• For the case $G(\cdot,\cdot)=G_2(\cdot,\cdot)$, its computability depends on the computability of $(\Pi\varphi_j,\varphi_i)_E$ and $(\Pi_E^0\Pi\varphi_j,\Pi_E^0\Pi\varphi_i)_E+\widetilde{S}^E((I-\Pi_E^0)\Pi\varphi_j,(I-\Pi_E^0)\Pi\varphi_i)$. In fact, the term $(\varphi_j,\varphi_i)_E$ of G_2 is easy to compute and the term $(\varphi_j,\Pi\varphi_i)_E$ is a transpose of the term $(\Pi\varphi_j,\varphi_i)_E$. If we consider the last identity in (5.1) and assume

$$\Pi\varphi_j=\sum_{\alpha=1}^{N_u} z_j^\alpha \psi_\alpha, \quad j=1,\cdots,N_p$$

with φ_j be the basis functions of the space Z_h, it holds

$$(\Pi\varphi_j,\varphi_i)_E \xlongequal{\text{def of } X_h} (\Pi_E^\nabla \Pi\varphi_j,\varphi_i)_E=\sum_{\alpha=1}^{N_u} z_j^\alpha(\Pi_E^\nabla\psi_\alpha,\varphi_i)_E=\sum_{\alpha=1}^{N_u}\sum_{\beta=1}^{n_k} z_j^\alpha s_\alpha^\beta(m_\beta,\varphi_i)_E,$$

whose corresponding matrix expressions should be $H_p(G^{-1}B)\mathbf{\Pi}$, i.e.,

$$\begin{pmatrix} (m_1,\varphi_1)_E & (m_2,\varphi_1)_E & \cdots & (m_{n_k},\varphi_1)_E \\ (m_1,\varphi_2)_E & (m_2,\varphi_2)_E & \cdots & (m_{n_k},\varphi_2)_E \\ \vdots & \vdots & \ddots & \vdots \\ (m_1,\varphi_{N_p})_E & (m_2,\varphi_{N_p})_E & \cdots & (m_{n_k},\varphi_{N_p})_E \end{pmatrix} (G^{-1}B) \begin{pmatrix} z_1^1 & z_2^1 & \cdots & z_{N_p}^1 \\ z_1^2 & z_2^2 & \cdots & z_{N_p}^2 \\ \vdots & \vdots & \ddots & \vdots \\ z_1^{N_u} & z_2^{N_u} & \cdots & z_{N_p}^{N_u} \end{pmatrix}. \tag{5.3}$$

Similarly, we have

$$\begin{aligned}&(\Pi_E^0\Pi\varphi_j,\Pi_E^0\Pi\varphi_i)_E+\widetilde{S}^E((I-\Pi_E^0)\Pi\varphi_j,(I-\Pi_E^0)\Pi\varphi_i)\\ =&\sum_{\alpha=1}^{N_u}\sum_{\beta=1}^{N_u} z_j^\alpha z_i^\beta\left[(\Pi_E^0\psi_\alpha,\Pi_E^0\psi_\beta)_E+\widetilde{S}^E((I-\Pi_E^0)\psi_\alpha,(I-\Pi_E^0)\psi_\beta)\right]\end{aligned}$$

and its corresponding matrix expression

$$\mathbf{\Pi}^T\left[C^TH^{-1}C+|E|(I-DH^{-1}C)^T(I-DH^{-1}C)\right]\mathbf{\Pi}.$$

Now, we can achieve the assembly of the local stiffness matrix (5.2) as soon as the matrix $\mathbf{\Pi}$ in (5.3) which is the coefficients of $\Pi\varphi_i$, $i=1,\cdots,N_p$ in the basis ψ_α, $\alpha=1,\cdots,N_u$ can be calculated. Actually, the choice of the operator $\Pi: L^2(\Omega)\to X_h$ has great flexibility (which is also an attractive feature of our stabilization method), that is to say, some operators satisfying two assumptions (2.11) and (2.12) can be used, such as virtual element projection or interpolation operators. From a practical point of view, the main factors in choosing Π are computational simplicity and locality (i.e., its computability can be achieved at the element level using only standard nodal data structures). With this in mind, there are two suitable choices of Π that can stabilize the lowest-order conforming virtual element pair:

(1) Virtual element solution: in this case, $\Pi\varphi_i:=v_h$ can be defined as a virtual element discrete solution of the equation $v=\varphi_i$, where φ_i is the piecewise constant on mesh partition $\mathcal{T}_h$. The action of the operator defined above can be computed and satisfies the properties (2.11) (c.f. [50]) and (2.12) (c.f. [18]).

Following the standard virtual element solving process, we know the local discrete bilinear and right-hand schemes of the equation $v=\varphi_i$ is

$$(\Pi_E^0 v,\Pi_E^0 w)_E+\widetilde{S}^E((I-\Pi_E^0)v,(I-\Pi_E^0)w)\quad\text{and}\quad(\varphi_i,\Pi_E^0 w)_E,$$

whose matrix form is

$$C^TH^{-1}C+|E|(I-DH^{-1}C)^T(I-DH^{-1}C)\quad\text{and}\quad(H^{-1}C)^T\begin{pmatrix}(\varphi_i,m_1)_E\\(\varphi_i,m_2)_E\\\vdots\\(\varphi_i,m_{n_k})_E\end{pmatrix}.$$

By assembling the global stiffness matrix and the discrete right-hand term, it is easy to obtain the i-th column of $\mathbf{\Pi}$. It is worth mentioning that we only need to assemble the global Stiffness matrix once and choose the matrix form of the global discrete right-hand term as

$$\begin{pmatrix}(\varphi_1,m_1)_{E_1}&(\varphi_2,m_1)_{E_2}&\cdots&(\varphi_{N_p},m_1)_{E_{N_p}}\\(\varphi_1,m_2)_{E_1}&(\varphi_2,m_2)_{E_2}&\cdots&(\varphi_{N_p},m_2)_{E_{N_p}}\\\vdots&&&\\(\varphi_1,m_{n_k})_{E_1}&(\varphi_2,m_{n_k})_{E_2}&\cdots&(\varphi_{N_p},m_{n_k})_{E_{N_p}}\end{pmatrix}$$

to get all the columns of $\mathbf{\Pi}$, where E_i, $i=1,\cdots,N_p$ represents the element of $\mathcal{T}_h$ on which the piecewise constant function φ_i is not zero.

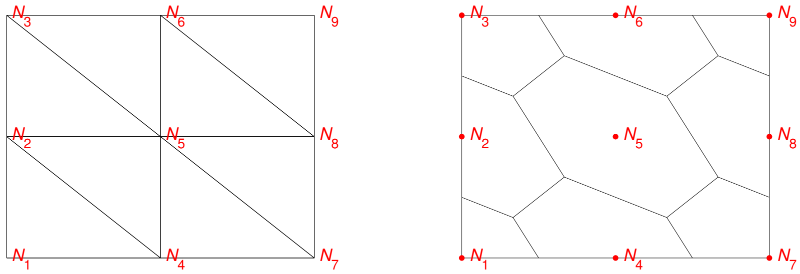

Figure 1: A patch of elements (left) and a dual volume (right) associated with the node $\mathcal{N}_i$.

(2) Clément-like interpolant: in this case, we set Π as Clément-like interpolant by using a projection onto the dual volume (instead of onto a patch of elements) associated with each node, see Fig. 1. In fact, this choice leads to a particularly simple formula (for the piecewise constant function φ_i) that does not require explicit construction of a dual cell, and satisfies the properties (2.11) and (2.12) (c.f. [44–46]).

More specifically, given a node $\mathcal{N}_\alpha$ in $\mathcal{T}_h$ and its dual volume $\widehat{\Omega}_\alpha$, the coefficients z_i^α of

$$\Pi\varphi_i = \sum_{\alpha=1}^{N_u} z_i^\alpha \psi_\alpha, \quad i=1,\cdots,N_p$$

are the constant function on $\widehat{\Omega}_\alpha$ that minimizes the functional

$$J_\alpha(\varphi_i) = \frac{1}{2}\int_{\widehat{\Omega}_\alpha} (z_i^\alpha - \varphi_i)^2 d\mathbf{x}.$$

For a piecewise constant function $\varphi_i \in L^2(\Omega)$, the functional $J_\alpha(\varphi_i)$ further simplifies to

$$J_\alpha(\varphi_i) = \sum_m \frac{1}{2}(z_i^\alpha - \varphi_i|_{E_m})^2 |E_m|,$$

where $|E_m|$ represents the area of E_m; $\varphi_i|_{E_m}$ represents the restriction of φ_i to E_m; and E_m represents the subcell of the dual volume (associated with the node $\mathcal{N}_\alpha$) that is formed by intersecting with the (original) mesh partition $\mathcal{T}_h$ and satisfies $\widehat{\Omega}_\alpha = \bigcup_m E_m$. Furthermore, minimization of $J_\alpha(\varphi_i)$ yields the formula

$$z_i^\alpha = \frac{\sum_m \varphi_i|_{E_m} |E_m|}{|\widehat{\Omega}_\alpha|} = \sum_m \varphi_i|_{E_m} \frac{|E_m|}{|\widehat{\Omega}_\alpha|}.$$

In fact, we can choose the dual volumes such that all E_m associated with the node $\mathcal{N}_\alpha$ are equal, which leads to the very simple case

$$z_i^\alpha = \sum_m \frac{\varphi_i|_{E_m}}{n_\alpha},$$

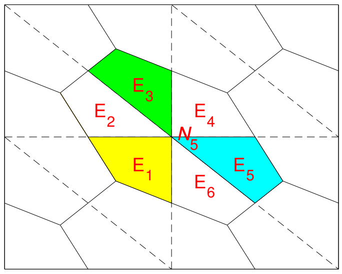

Figure 2: An example of E_m, $m=1,\cdots,6$ associated with the node $\mathcal{N}_5$.

where n_α is the number of all subcell of the dual volume (associated with the node $\mathcal{N}_\alpha$). Taking the case in Fig. 1 as an example, for the node $\mathcal{N}_5$ in $\mathcal{T}_h$ and its dual volume $\widehat{\Omega}_5$, we know that E_m, $m=1,\cdots,6$ is shown in Fig. 2 and the coefficients are

$$z_i^5=\frac{|E_1|}{|\widehat{\Omega}_5|}\varphi_i|_{E_1}+\frac{|E_2|}{|\widehat{\Omega}_5|}\varphi_i|_{E_2}+\cdots+\frac{|E_6|}{|\widehat{\Omega}_5|}\varphi_i|_{E_6}.$$

That is to say, for the piecewise constant φ_1, it holds $z_1^5=0$ due to the fact that $\varphi_1|_{E_m}=0$, $m=1,\cdots,6$; for the piecewise constant φ_2, it holds $z_2^5=\frac{|E_1|}{|\widehat{\Omega}_5|}$ due to the fact that $\varphi_2|_{E_1}=1$ and $\varphi_2|_{E_m}=0$, $m=2,\cdots,6$; for the piecewise constant φ_3, it holds $z_3^5=\frac{|E_6|}{|\widehat{\Omega}_5|}$ due to the fact that $\varphi_3|_{E_6}=1$ and $\varphi_3|_{E_m}=0$, $m=1,\cdots,5$; the remaining coefficients can be similarly obtained.

6 Numerical examples

In this section, in order to verify the H^1- and L^2-convergence rates for the lowest-order pairs in two and three space dimensions, we report some numerical results obtained by using the stabilized method based on the local pressure jumps or projection stabilization term. The following error norms are used for the investigation of convergence rates:

$$\begin{aligned}
||e_{\mathbf{u},h}||_0&=\sqrt{\sum_{E\in\mathcal{T}_h}||\mathbf{u}-\Pi_0^E\mathbf{u}_h||_{0,E}^2}=\sqrt{\sum_{E\in\mathcal{T}_h}\sum_{i=1}^d\int_E(\mathbf{u}_i-\Pi_0^E\mathbf{u}_{hi})^2d\mathbf{x}},\\
||e_{\mathbf{u},h}||_1&=\sqrt{\sum_{E\in\mathcal{T}_h}|\mathbf{u}-\Pi_0^E\mathbf{u}_h|_{1,E}^2}=\sqrt{\sum_{E\in\mathcal{T}_h}\sum_{i=1}^d\int_E\nabla(\mathbf{u}_i-\Pi_0^E\mathbf{u}_{hi})\cdot\nabla(\mathbf{u}_i-\Pi_0^E\mathbf{u}_{hi})d\mathbf{x}},\\
||e_{p,h}||_0&=\sqrt{\sum_{E\in\mathcal{T}_h}||p-p_h||_{0,E}^2}=\sqrt{\sum_{E\in\mathcal{T}_h}\int_E(p-p_h)^2d\mathbf{x}},
\end{aligned}$$

where d denotes the spatial dimension and $\mathbf{v}_i$, $i=1,\cdots,d$, denote the components of the vector $\mathbf{v}$ ($\mathbf{v}=\mathbf{u}$ or $\mathbf{u}_h$).

6.1 2D test problem

In this example, we select $\nu=1$, the unit square domain Ω and a pair of smooth functions

$$\mathbf{u}=\begin{pmatrix} \pi\sin(\pi x)\sin(\pi x)\sin(2\pi y) \\ -\pi\sin(\pi y)\sin(\pi y)\sin(2\pi x) \end{pmatrix}, \quad p=\cos(\pi x)\cos(\pi y),$$

with p having zero mean (that is, the constraint $\int_\Omega p_h \, d\mathbf{x}=0$ should be imposed), which help to decide the source term $\mathbf{f}$ and the boundary data. Also, four different types of meshes are employed in Fig. 3: triangular mesh $\mathcal{T}_h^1$, randomly distorted quadrilateral mesh $\mathcal{T}_h^2$, non-structured hexagonal mesh $\mathcal{T}_h^3$, non-convex mesh $\mathcal{T}_h^4$.

The error results and convergence orders of two stabilized lowest-order virtual elements for both velocity and pressure are shown in Figs. 4-6, respectively. We observe that the H^1-convergence order of the velocity and the L^2-convergence order of the pressure are $\mathcal{O}(h)$ and the L^2-convergence order of the velocity is $\mathcal{O}(h^2)$, which is consistent with the theoretical analysis in all cases.

Furthermore, to test the impact of stabilization parameter δ from G_1 on error results, we also illustrate the convergence of the method on the triangular mesh $\mathcal{T}_h^1$ with stabilization parameters $\delta=0.001,0.01,0.1,1,10,100,1000$ in Fig. 7. Obviously, from the error results of velocity and pressure, it can be seen that when the value of δ is too large (10,100,1000) or too small (0.001), it will lead to inaccurate convergence results (this is an interesting phenomenon, but it is beyond the scope of our manuscript). For this two-dimensional example, a more reasonable choice may be $\delta=1$.

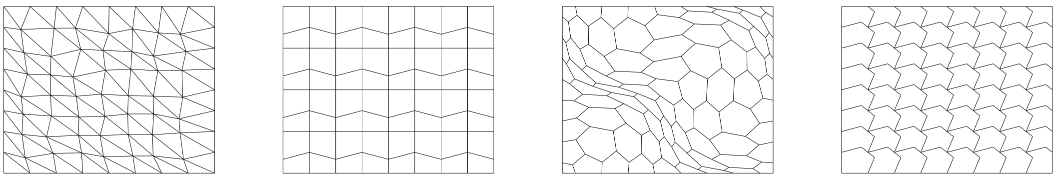

Figure 3: Four mesh families for the 2D convergence test.

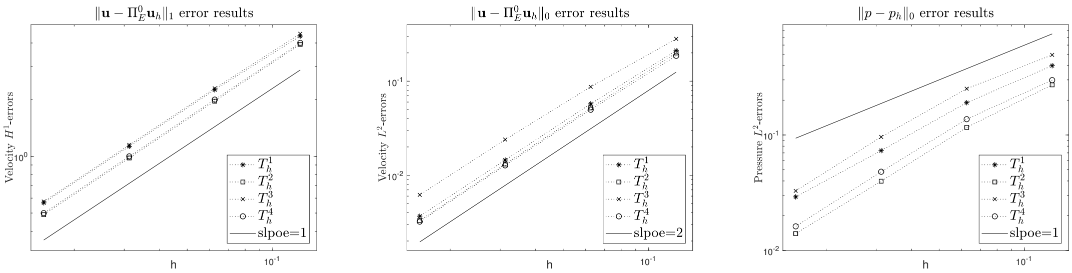

Figure 4: Convergence results for the two-dimensional example based on the local pressure jump stabilization with $\delta=1$.

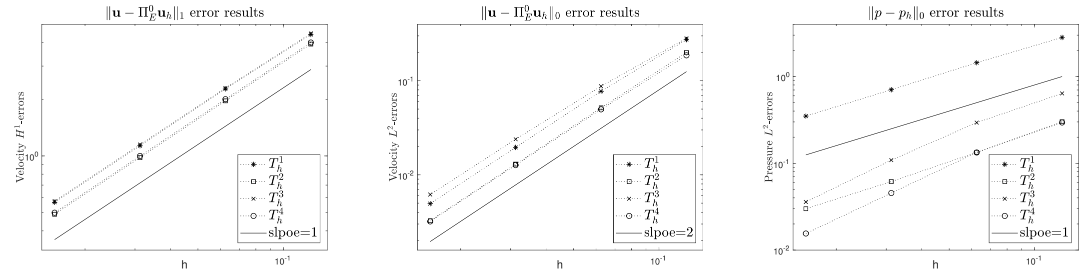

Figure 5: Convergence results for the two-dimensional example based on the local pressure projection stabilization where Π is a Clément-like interpolant.

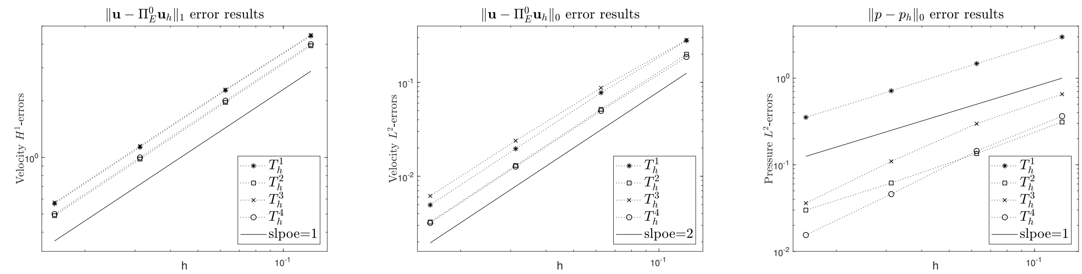

Figure 6: Convergence results for the two-dimensional example based on the local pressure projection stabilization where Π is a virtual element solution.

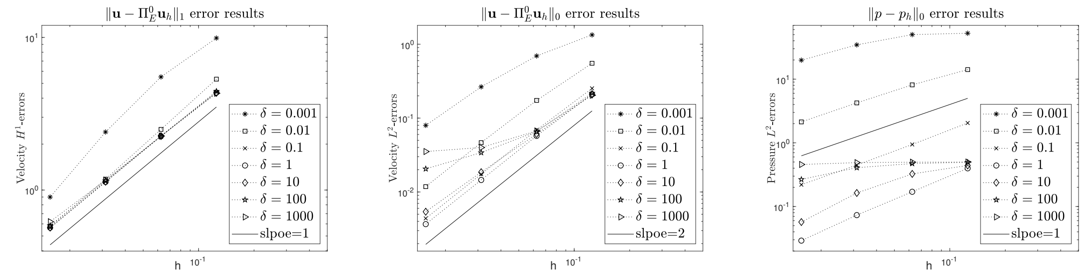

Figure 7: Convergence results on triangular mesh $\mathcal{T}_h^1$ with different local pressure jump stabilization parameters $\delta=0.001,0.01,0.1,1,10,100,1000$.

6.2 3D test problem

Extending the test problem in Example 6.1 to the unit cube, we set

$$
\begin{aligned}
&\mathbf{u}=\begin{pmatrix} x^2(x-1)^2\big(2y(y-1)(2y-1)z^2(z-1)^2-2y^2(y-1)^2z(z-1)(2z-1)\big)\\ y^2(y-1)^2\big(2z(z-1)(2z-1)x^2(x-1)^2-2z^2(z-1)^2x(x-1)(2x-1)\big)\\ z^2(z-1)^2\big(2x(x-1)(2x-1)y^2(y-1)^2-2x^2(x-1)^2y(y-1)(2y-1)\big)\end{pmatrix},\\
&p=\cos(\pi x)\cos(\pi y)\sin(\pi z).
\end{aligned}
$$

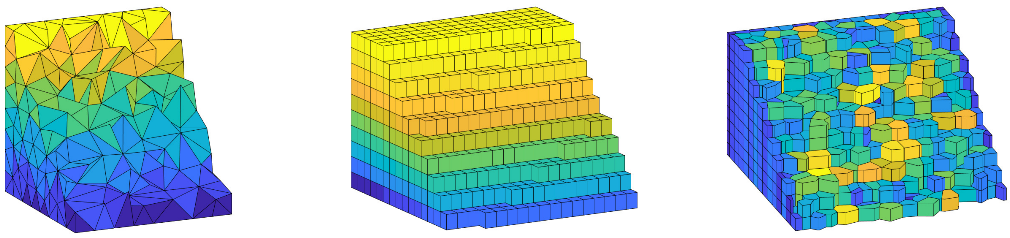

Figure 8: Tetrahedral, hexahedral and polyhedral mesh families for the 3D convergence test.

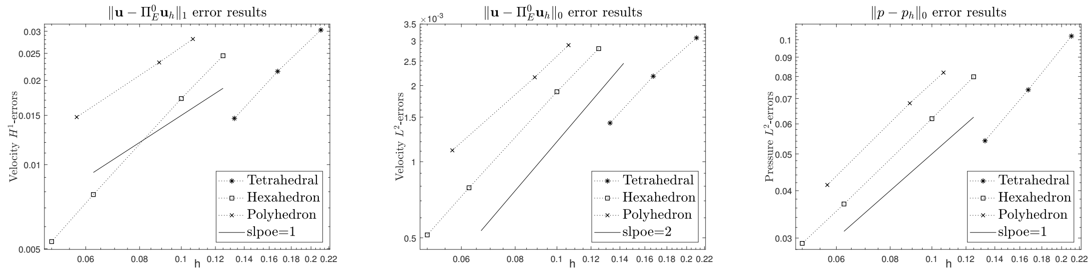

Figure 9: Convergence results for the three-dimensional example based on the local pressure jump stabilization with $\delta = 0.1$.

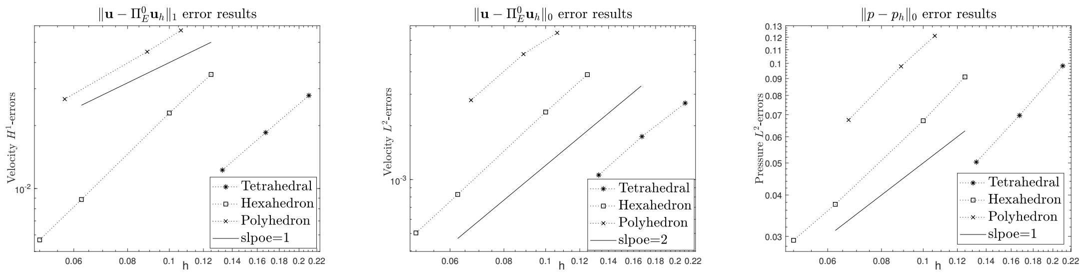

Figure 10: Convergence results for the three-dimensional example based on the local pressure projection stabilization where Π is a Clément-like interpolant.

The values of $\mathbf{f}$ and $\mathbf{u}$ on the boundary of the cube are constrained to those given by the above solution. And the tetrahedral, hexahedral and polyhedral meshes used in this numerical test are shown in Fig. 8.

The rates of convergence for the velocity and pressure in the appropriate norm are illustrated in Figs. 9-11. As was the case for the two-dimensional example, the theoretical convergence rates are confirmed, and the H^1-convergence results of the velocity on hexahedral meshes are higher than $\mathcal{O}(h)$, which may be caused by the specificity of the mesh partition. Moreover, for this three-dimensional example, it is better to choose a (com-

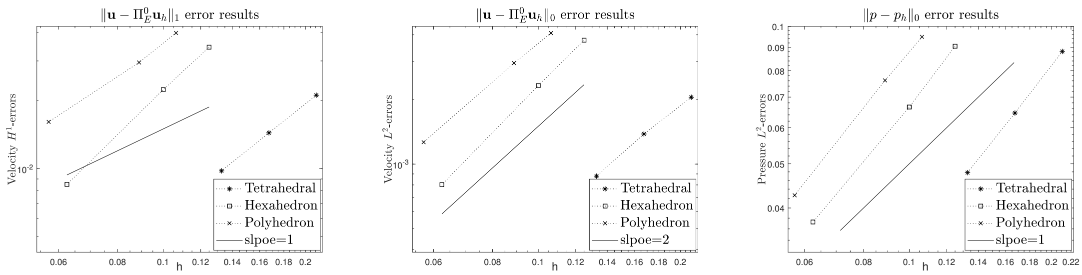

Figure 11: Convergence results for the three-dimensional example based on the local pressure projection stabilization where Π is a virtual element solution.

pared to the two-dimensional case) smaller $\delta=0.1$ (instead of $\delta=1$) for the stabilization parameter of the local pressure jump stabilization.

Acknowledgments

This research was supported in part by National Natural Science Foundation of China (No. 12371405) and General items of Shaanxi Railway Institute (No. 2023KYYB-06).

References

[1] M. Crouzeix, and P. A. Raviart, Conforming and nonconforming finite element methods for solving the stationary Stokes equations, RAIRO Serie Rouge, 7 (1973), pp. 33-75.

[2] R. Rannacher, and S. Turek, Simple nonconforming quadrilateral Stokes element, Numer Methods Partial Differential Eq., 8 (1992), pp. 97-111.

[3] Z. Cai, C. Tong, P. S. Vassilevski, and C. Wang, Mixed finite element methods for incompressible flow: Stationary Stokes equations, Numer Methods Partial Differential Eq., 26 (2010), pp. 957-978.

[4] D. J. Silvester, and N. Kechkar, Stabilized bilinear-constant velocity-pressure finite elements for the conjugate gradient solution of the Stokes Problem, Comput. Methods Appl. Mech. Engrg., 79 (1990), pp. 71-86.

[5] F. Brezzi, On existence, uniqueness, and approximation of saddle-point problems arising from Lagrangian multipliers, RAIRO Model. Math. Anal. Numer., 21 (1974), pp. 129-151.

[6] T. J. R. Hughes, W. Liu, and A. Brooks, Finite element analysis of incompressible viscous flows by the penalty function formulation, J. Comput. Phys., 30 (1979), pp. 1-60.

[7] C. Johnson, and J. Pitkaranta, Analysis of some mixed finite element methods related to reduced integration, Math. Comp., 38 (1982), pp. 375-400.

[8] T. J. Oden, RIP-methods for Stokesian flow, in Finite Elements in Fluids, Vol. 4, R. H.Gallagher, D. H. Norrie, J. T. Oden, and O. C. Zienkiewicz, eds., John Wiley, New York, (1982), pp. 305-318.

[9] T. Barth, P. Bochev, M. Gunzburger, and J. Shadid, A taxonomy of consistently stabilized finite element methods for the Stokes problem, SIAM J. Sci. Comput., 25 (2004), pp. 1585-1607.

[10] M. Behr, L. Franca, and T. Tezduyar, Stabilized finite element methods for the velocity-pressure-stress formulation of incompressible flows, Comput. Methods Appl. Mech. Engrg., 104 (1993), pp. 31-48.

[11] J. Blasco, and R. Codina, Stabilized finite element method for the transient Navier-Stokes equations based on a pressure gradient projection, Comput. Methods Appl. Mech. Engrg., 182 (2000), pp. 277-300.

[12] J. Blasco, and R. Codina, Space and time error estimates for a first-order, pressure stabilized finite element method for the incompressible Navier-Stokes equations, Appl. Numer. Math., 38 (2001), pp. 475-497.

[13] R. Codina, and J. Blasco, Analysis of a pressure stabilized finite element approximation of the stationary Navier-Stokes equations, Numer. Math., 87 (2000), pp. 59-81.

[14] R. Becker, and M. Braack, A finite element pressure gradient stabilization for the Stokes equations based on local projections, Calcolo, 38 (2000), pp. 173-199.

[15] J. Li, and Y. N. He, A stabilized finite element method based on two local Gauss integrations for the Stokes equations, J. Comput. Appl. Math., 214 (2008), pp. 58-65.

[16] C. Dohrmann, and P. Bochev, A stabilized finite element method for the Stokes problem based on polynomial pressure projections, Int. J. Numer. Methods Fluids, 46 (2004), pp. 183-201.

[17] P. B. Bochev, C. R. Dohrmann, and M. D. Gunzburger, Stabilization of low-order mixed finite elements for the Stokes equations. SIAM J. Numer. Anal., 44 (2006), pp. 82-101.

[18] L. Beirão da Veiga, F. Brezzi, A. Cangiani, G. Manzini, L. D. Marini, and A. Russo, Basic principles of virtual element methods, Math. Models Methods Appl. Sci., 23 (2013), pp. 199-214.

[19] L. Beirão da Veiga, F. Brezzi, L.D. Marini, and A. Russo, The hitchhiker's guide to the virtual element method, Math. Models Methods Appl. Sci., 24 (2014), pp. 1541-1573.

[20] B. Ahmed, A. Alsaedi, F. Brezzi, L. D. Marini, and A. Russo, Equivalent projectors for virtual element methods, Comput. Math. Appl., 66 (2013), pp. 376-391.

[21] L. Beirão da Veiga, and G. Manzini, A virtual element method with arbitrary regularity, IMA J. Numer. Anal., 34 (2014), pp. 759-781.

[22] F. Brezzi, and L. D. Marini, Virtual element method for plate bending problems, Comput. Methods Appl. Mech. Engrg., 253 (2012), pp. 455-462.

[23] B. Ayuso de Dios, K. Lipnikov, and G. Manzini, The nonconforming virtual element method, ESAIM Math. Model. Numer. Anal., 50 (2016), pp. 879-904.

[24] A. Cangiani, G. Manzini, and O. J. Sutton, Conforming and nonconforming virtual element methods for elliptic problems, IMA J. Numer. Anal., 37 (2017), pp. 1317-1354.

[25] L. Beirão da Veiga, F. Brezzi, L. D. Marini, and A. Russo, $H(\mathrm{div})$ and $H(\mathrm{curl})$-conforming virtual element methods, Numer. Math., 133 (2016), pp. 303-332.

[26] F. Brezzi, R. S. Falk, and L. D. Marini, Basic principles of mixed virtual element methods, ESAIM Math. Model. Numer. Anal., 48 (2014), pp. 1227-1240.

[27] A. Cangiani, E. H. Georgoulis, T. Pryer, and O. J. Sutton, A posteriori error estimates for the virtual element method, Numer. Math., 137 (2017), pp. 857-893.

[28] M. Frittelli, A. Madzvamuse, and I. Sgura, Virtual element method for elliptic bulk-surface PDEs in three space dimensions, Numer Methods Partial Differential Eq., 39 (2023), pp. 4221-4247.

[29] L. Beirão da Veiga, F. Brezzi, and L. D. Marini, Virtual elements for linear elasticity problems, SIAM J. Numer. Anal., 51 (2013), pp. 794-812.

[30] D. Y. Kwak, and H. Park, Lowest-order virtual element methods for linear elasticity prob-

lems, Comput. Methods Appl. Mech. Eng., 390 (2022), Article 114448.
[31] P. F. Antonietti, L. Beirão da Veiga, D. Mora, and M. Verani, A stream virtual element formulation of the Stokes problem on polygonal meshes, SIAM J. Numer. Anal., 52 (2014), pp. 386-404.
[32] L. Beirão da Veiga, C. Lovadina, and G. Vacca, Divergence free virtual elements for the Stokes problem on polygonal meshes, ESAIM Math. Model. Numer. Anal., 51 (2017), pp. 509-535.
[33] X. Liu, J. Li, and Z. X. Chen, A nonconforming virtual element method for the Stokes problem on general meshes, Comput. Methods Appl. Mech. Engrg., 320 (2017), pp. 694-711.
[34] D. Frerichs, and C. Merdon, Divergence-preserving reconstructions on polygons and a really pressure-robust virtual element method for the Stokes problem, IMA J. Numer. Anal., 42 (2022), pp. 597-619.
[35] G. Wang, Y. Wang, and Y. N. He, A posteriori error estimates for the virtual element method for the Stokes problem, J. Sci. Comput., 84 (2020), Article 37.
[36] J. Meng, L. Beirão da Veiga, and L. Mascotto, Stability and interpolation properties for Stokes-like virtual element spaces, J. Sci. Comput., 94 (2023), Article 56.
[37] J. Guo, and M. Feng, A new projection-based stabilized virtual element method for the Stokes problem, J. Sci. Comput., 85 (2020), Article 16.
[38] Y. Li, C. Hu, and M. Feng, A least-squares stabilization virtual element method for the Stokes problem on polygonal meshes, Int. J. Numer. Anal. Mod., 19 (2022), pp. 685-708.
[39] D. Irisarri, and G. Hauke, Stabilized virtual element methods for the unsteady incompressible Navier-Stokes equations, Calcolo, 56 (2019), pp. 1-21.
[40] Y. Li, M. F. Feng, and Y. Luo, A new local projection stabilization virtual element method for the Oseen problem on polygonal meshes, Adv. Comput. Math., 48 (2022), Article 30.
[41] M. F. Benedetto, S. Berrone, A. Borio, S. Pieraccini, and S. Scialò, Order preserving SUPG stabilization for the virtual element formulation of advection-diffusion problems, Comput. Methods Appl. Mech. Engrg., 311 (2016), pp. 18-40.
[42] S. Berrone, A. Borio, and G. Manzini, SUPG stabilization for the nonconforming virtual element method for advection-diffusion-reaction equations, Comput. Methods Appl. Mech. Engrg., 340 (2018), pp. 500-529.
[43] M. Frittelli, A. Madzvamuse, and I. Sgura, The bulk-surface virtual element method for reaction-diffusion PDEs: analysis and applications, Commun. Comput. Phys., 33 (2023), pp. 733-763.
[44] V. Girault, and P. Raviart, Finite Element Methods for Navier-Stokes Equations, Springer Series in Computational Mathematics. Springer-Verlag, Berlin (1986).
[45] Z. Chen, Finite Element Methods and Their Applications, Springer-Verlag, Heidelberg and New York (2005).
[46] Z. Chen, BDM mixed methods for a nonlinear elliptic problem, J. Comp. Appl. Math. 53 (1994), pp. 207-223.
[47] L. Mascotto, The role of stabilization in the virtual element method: A survey, Comput. Math. Appl., 151 (2023), pp. 244-251.
[48] E. Burman, and P. Hansbo, A unified stabilized method for Stokes' and Darcy's equations, J. Comput. Appl. Math., 198 (2007), pp. 35-51.
[49] P. G. Ciarlet, The Finite Element Method for Elliptic Problems, Classics in Applied Mathematics. Society for Industrial and Applied Mathematics, Philadelphia (2002).
[50] L. Chen, and J. Huang, Some error analysis on virtual element methods, Calcolo, 55 (2018), pp. 1-23.
[51] L. Beirão da Veiga, L. B. Brezzi, F. Brezzi, L. D. Marini, and A. Russo, Mixed virtual ele-

ment methods for general second order elliptic problems on polygonal meshes, ESAIM Math. Model. Numer. Anal., 50 (2016), pp. 727-747.

[52] D. Mora, G. Rivera, and R. Rodrguez, A virtual element method for the Steklov eigenvalue problem, Math. Models Methods Appl. Sci., 25 (2015), pp. 1421-1445.

[53] S. C. Brenner, and L. Sung, Virtual element methods on meshes with small edges or faces, Math. Models Methods Appl. Sci., 28 (2018), pp. 1291-1336.

[54] A. Allendes, G. R. Barrenechea, and A. Novo, A divergence-free stabilized finite element method for the evolutionary Navier-stokes equations, SIAM J. Sci. Comput., 43 (2021), pp. A3809-A3836.